

Guiding What *Not* to Generate: Automated Negative Prompting for Text-Image Alignment

Sangha Park¹ Eunji Kim² Yeongtak Oh¹ Jooyoung Choi¹ Sungroh Yoon^{1,3†}

¹Department of Electrical and Computer Engineering, Seoul National University, ²Amazon

³IPAI, AIIS, ASRI, INMC, and ISRC, Seoul National University

Abstract

*Despite substantial progress in text-to-image generation, achieving precise text-image alignment remains challenging, particularly for prompts with rich compositional structure or imaginative elements. To address this, we introduce **Negative Prompting for Image Correction (NPC)**, an automated pipeline that improves alignment by identifying and applying negative prompts that suppress unintended content. We begin by analyzing cross-attention patterns to explain why both targeted negatives—those directly tied to the prompt’s alignment error—and untargeted negatives—tokens unrelated to the prompt but present in the generated image—can enhance alignment. To discover useful negatives, NPC generates candidate prompts using a verifier-captioner-proposer framework and ranks them with a salient text-space score, enabling effective selection without requiring additional image synthesis. On GenEval++ and Imagine-Bench, NPC outperforms strong baselines, achieving 0.571 vs. 0.371 on GenEval++ and the best overall performance on Imagine-Bench. By guiding what not to generate, NPC provides a principled, fully automated route to stronger text-image alignment in diffusion models. Code is released at <https://github.com/wiaerae/NPC>.*

1. Introduction

Text-to-image (T2I) generation has surged with the proliferation of large-scale diffusion models [22, 48]—including Stable Diffusion [11, 49, 54], DALL-E 3 [3], and FLUX [26]—which have revolutionized content creation by enabling diverse, photorealistic images from natural language. Despite these advances, models still frequently fail to satisfy prompt alignment in practice, particularly for prompts with rich compositional structure (multiple objects, attributes, relations, and counts) [18, 28] and surreal instructions (e.g., a square soccer ball) [21, 45].

To improve alignment, recent work has explored self-correction via iterative critique-and-revision [5], fine-tuning with large-scale synthetic alignment data [75], and chain-of-thought-based prompt rewriting [59]. These methods primarily focus on *positive guidance* in the classifier-free guidance (CFG) sense—that is, strengthening conditioning on the desired content.

Complementing these positive-guidance approaches, a parallel strategy improves alignment by explicitly telling the model what not to generate—suppressing or removing interfering content. Prior efforts typically exhibit two characteristics: (i) layout-centric pipelines [32, 66], which constrain element placement by pruning objects, attributes, and spatial relations, but often at the cost of realism due to rigid or imperfect layouts [46, 76]; and (ii) methods addressing **targeted** misalignments [66, 73], suppressing elements that contradict the positive prompt (e.g., “one laptop” when three laptops are requested; see Figure 1).

Instead of relying on explicit layouts, *negative guidance* (in the CFG sense) can discourage the generation of particular content, alleviating realism issues. From this perspective, beyond such targeted misalignments, there exist other candidates for negative prompts—details that appear in the image generated from the positive prompt but do not directly harm alignment (which we refer to as **untargeted** negatives, e.g., a “wooden table”)—whose impact on alignment, to our knowledge, has not been systematically analyzed. To address the lack of systematic analysis of untargeted negatives and of their combination with targeted negatives, we propose a pipeline to **discover effective negative prompts that enhance alignment** when used as negative guidance.

Moving beyond conventionally used, quality-oriented negatives (e.g., “low quality,” “blurry”), we consider a broader class of negative prompts consisting of both *targeted* and *untargeted* variants. In Section 3, we analyze their effect on alignment from a transformer-attention perspective. We compute image-text cross-attention from the denoising latents to the positive-prompt tokens across dif-

†Corresponding author

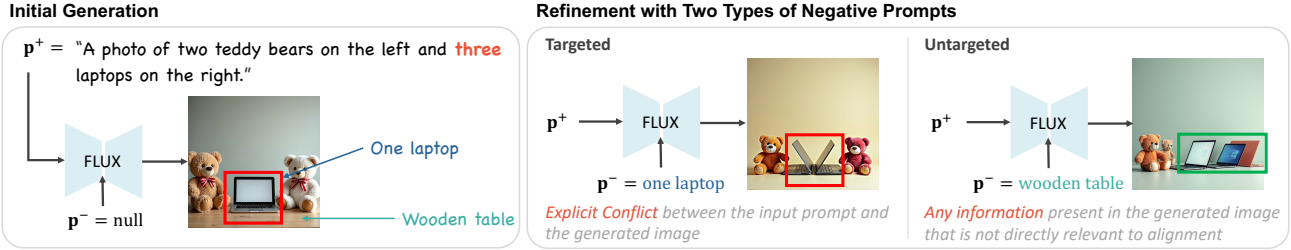


Figure 1. Example of two types of negative prompts used for CFG-based negative guidance: targeted negatives (directly tied to alignment errors) and untargeted negatives (not explicitly related to alignment but appearing in the generated image). Although targeted negatives directly address the error, they do not always ensure alignment, whereas untargeted negatives may still succeed in improving it.

fusion timesteps and show that introducing either type of negative guidance increases the attention allocated to salient tokens in the positive prompt. However, identifying which negatives will be effective for a given prompt–image pair remains nontrivial, making naïve trial-and-error regeneration expensive and motivating the need for an automated selection mechanism.

Building on this, we introduce **NPC**, an automated pipeline that minimizes generation trials: (i) it generates multiple candidate negative prompts via a verifier–captioner–proposer framework, and (ii) uses a *salient score* to select the most effective negative prompt, achieving alignment with only a few on-image trials (see Figure 3). Concretely, NPC works in four steps. First, the *verifier* checks an image created from the original prompt; if the image is misaligned, it points out specific failure reasons, which we treat as **targeted** negatives. Second, the *captioner* describes the image in natural language, and these captions provide **untargeted** negatives. Third, the *proposer* combines the *verifier*’s failure reasons with the captions to form several negative-prompt candidates. Finally, we score these candidates with a *salient score*—a text-based measure of how strongly each negative prompt is expected to contribute to improving alignment. Prioritizing the highest-scored candidate identifies an effective negative and reduces the number of regeneration attempts.

We validate NPC on two challenging benchmarks—GenEval++ [75], which emphasizes compositional control, and Imagine-Bench [75], which evaluates surreal transformations while preserving identity. Across both benchmarks, our approach outperforms strong contemporary T2I baselines. On GenEval++, NPC attains an overall score of 0.571, surpassing the strongest baseline Bagel [10], which scores 0.371, by 0.200—a relative gain of about 54%. On Imagine-Bench, NPC likewise achieves the best overall performance among baselines. Ablation studies further confirm the effectiveness of NPC. Our contributions are:

1. We expand the scope of negative prompting beyond conventional usage and provide an attention-based analysis

of how these negative prompts improve alignment.

2. We propose an automated pipeline for the generation and selection of negative prompts, thereby reducing manual prompting and human intervention.
3. We demonstrate superior performance on two challenging benchmarks, consistently exceeding state-of-the-art text-to-image models.

2. Related work

2.1. Text-to-Image Diffusion Models

Diffusion models [17, 57] generate data from noise and have become a strong image-generation paradigm thanks to stable training and scalability [11, 54]. GLIDE [42] first extended diffusion to text-to-image using CLIP embeddings [51] and classifier-free guidance [16]. Imagen [55] underscored the value of richer text encoders (T5 [9]), and recent systems like DALL-E 3 [3] and Stable Diffusion 3 [11] show that MLLM-synthesized captions [1] help with long, complex prompts.

Recent work increasingly pursues *unified multimodal generators* that couple understanding and generation within a single architecture (e.g., Show-o, Transfusion, BLIP3-o, Bagel, OmniGen2, Janus-Pro) [6, 7, 10, 65, 70, 77]. Whereas most efforts enrich the prompt or strengthen instruction following, we take a complementary direction: we design *effective negative prompts* that selectively suppress off-target content while preserving the intended semantics.

2.2. Text-Image Alignment

Alignment methods Recent work has improved compositional T2I generation across attribute binding, object relations, numeracy, and complex prompts [13, 37, 63, 76]. Approaches refine cross-attention to strengthen text alignment [4, 53], impose or predict layouts to control relations [30, 32, 61, 69, 73], and leverage MLLMs or human/reward feedback for compositionality and fidelity [8, 12, 19, 20, 23, 33, 35, 39, 56, 67, 71, 74].

Targeted corrections Many methods pursue *targeted* fixes—identifying specific errors in a generated image and editing them (e.g., attribute repair or object adjustment) using editing-capable models [66, 73]. Relatedly, several prompt-optimization approaches also rely on feedback from LLMs or MLLMs that explicitly surfaces which parts of the prompt fail to meet the desired alignment, driving the optimization through targeted correction at each step [25, 58].

Multi-turn generation Several methods adopt iterative, multi-turn pipelines to better match user intent: SLD [66] proposes coordinate and attribute edits, GenArtist [64] performs verification and self-correction with an MLLM, PASTA [41] optimizes preferences via RL, and T2I-Copilot [5] uses an MLLM-based evaluation agent with optional human-in-the-loop control. NPC follows this multi-turn refinement paradigm by leveraging negative prompts to guide regeneration toward improved alignment.

3. The Role of Negative Prompts

In this section, we examine how negative prompting affects text–image alignment. We first describe its mechanism within T2I models through the CFG formulation (Section 3.1), then introduce an attention-based score for quantifying its impact (Section 3.2). Using this score, we show that both targeted and untargeted negative prompts contribute to improved alignment (Section 3.3).

3.1. Negative Prompting in T2I Models

Modern diffusion- and flow-based text-to-image models [11, 36, 38, 49, 54] produce, at each timestep t , a prediction signal $f_\theta(x_t, c, t)$, conditioned on text c , a formulation that encompasses noise prediction (diffusion), velocity prediction (flow-matching), and score prediction within a single unified expression.

Let p denote the *positive* prompt and n the *negative* (or unconditional) prompt. Classifier-free guidance (CFG) forms a guided estimate by contrasting the positive branch with a null-conditioned branch:

$$\hat{f}_t = f_\theta(x_t, n, t) + \lambda \left(f_\theta(x_t, p, t) - f_\theta(x_t, n, t) \right), \quad (1)$$

where λ is the guidance scale. Replacing this null-conditioning with an explicit negative prompt preserves the classical CFG structure while enabling direct suppression of undesired concepts. The latent is then updated through a generic sampler Φ_t , yielding $x_{t-1} = \Phi_t(x_t, \hat{f}_t)$.

3.2. Measuring Cross-Attention Allocation

Our objective is to quantify how negative prompting alters the allocation of attention toward the semantics of the positive prompt. To this end, we separate the roles of queries and keys in the text–image cross-attention layers of

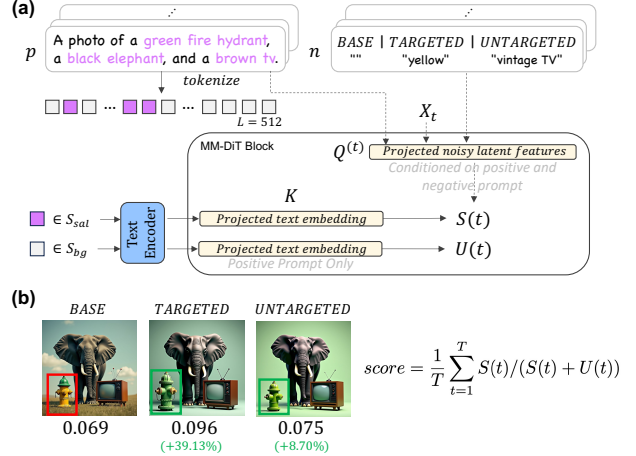


Figure 2. Analysis of how negative prompts influence alignment. (a) shows that cross-attention is computed with positive-prompt keys and latents (queries) influenced by both prompts. (b) shows that both negative prompts increase attention to salient tokens over BASE, illustrating their alignment-improving effect. Additional illustrative prompt examples are provided in Section C.

Transformer-based backbones used in diffusion and flow-matching models (e.g., DiT architectures [27, 47]).

Cross-attention After applying the guided update in Equation (1), we extract image-stream hidden states $H^{(t)} = \text{ImgEnc}(x_{t-1})$, which serve as the cross-attention queries and encode the influence of both the positive and negative prompts. To keep the text-side conditioning fixed, we obtain token embeddings of the positive prompt $E(p) \in \mathbb{R}^{L \times d_e}$ and form keys as $K^{\text{cond}} = W_k E(p)$. The queries, in contrast, evolve with the latent trajectory through $Q^{(t)} = W_q H^{(t)}$. For batch index b , head h , spatial position q , and token index k , the attention logit is

$$s_{b,h,q,k}^{(t)} = \frac{Q_{b,h,q}^{(t)} \cdot K_{b,h,k}^{\text{cond}}}{\sqrt{d_h}}. \quad (2)$$

Softmax over tokens yields the attention probabilities:

$$P_{b,h,q,k}^{(t)} = \frac{\exp(s_{b,h,q,k}^{(t)})}{\sum_j \exp(s_{b,h,q,j}^{(t)})}. \quad (3)$$

Salient-attention score Let $\mathcal{S}_{\text{sal}} \subset \{1, \dots, L\}$ be the set of salient tokens in the positive prompt—those corresponding to semantic elements that directly determine alignment quality (e.g., objects or their attributes). The remaining tokens form \mathcal{S}_{bg} . Since proper alignment requires the model to allocate sufficient attention to these salient tokens, an increase in their attention share reflects improved semantic grounding. We aggregate cross-attention mass over batch,

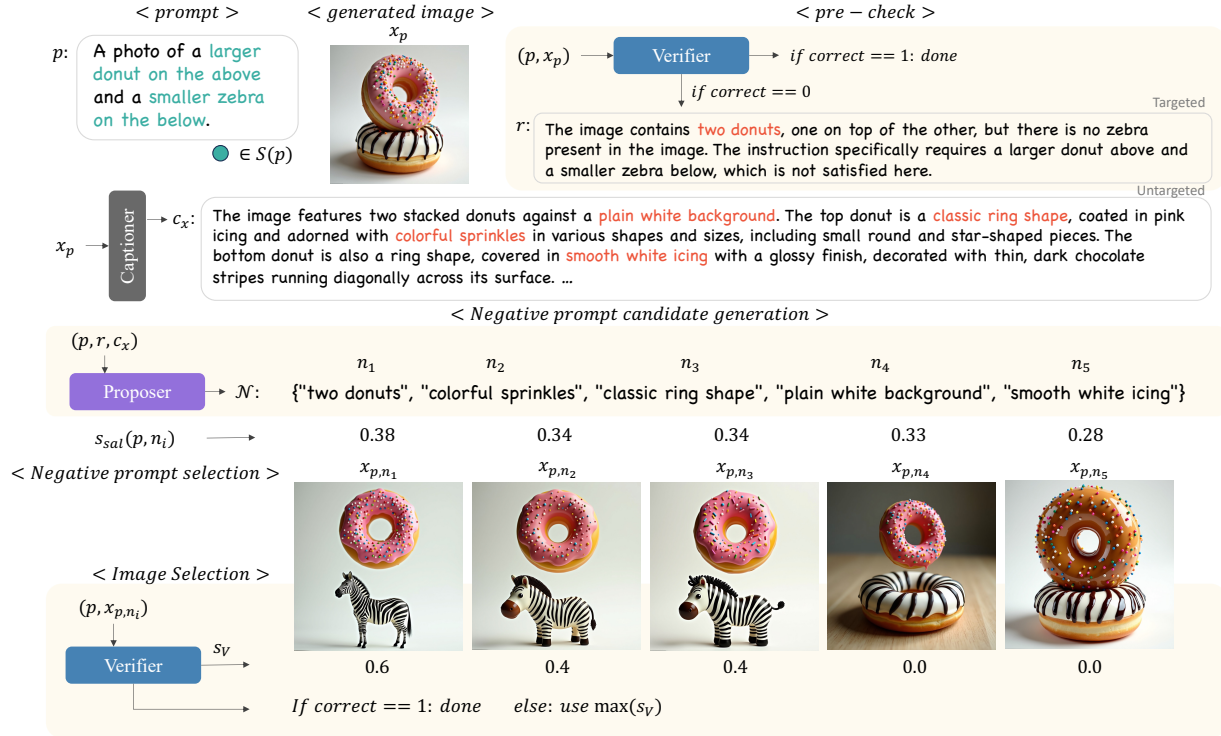


Figure 3. NPC overview. NPC runs an iterative generate–evaluate–refine loop: (i) a verifier judges each generated image and, if incorrect, produces a failure reason; (ii) a captioner generates a caption; (iii) the failure reason and caption condition a proposer to propose negative-prompt candidates; (iv) each candidate receives a salient score; candidates are applied in descending score order to regenerate images; verification is repeated, terminating upon a correct result or, if none are correct, selecting the sample with the highest verifier score.

heads, and spatial positions:

$$S(t) = \sum_{b,h,q} \sum_{k \in \mathcal{S}_{sal}} P_{b,h,q,k}^{(t)}, \quad U(t) = \sum_{b,h,q} \sum_{k \in \mathcal{S}_{bg}} P_{b,h,q,k}^{(t)}.$$

The *salient-attention score* is then defined as

$$\rho_{sal} = \frac{1}{T} \sum_{t=1}^T \frac{S(t)}{S(t) + U(t)} \quad (4)$$

where T denotes the total number of denoising steps. This score reflects how much of the model’s cross-attention is allocated to alignment-critical tokens. Since keys come from the positive prompt and only queries change under negative prompting, variations in ρ_{sal} reveal how negative prompts shift the model’s semantic focus throughout the denoising process.

3.3. Analysis Result

For the prompt “A photo of a *green* fire hydrant, a black elephant, and a brown tv,” we first generate an image using the BASE configuration, which applies no negative prompt. As shown in Figure 2(b), the hydrant appears *yellow* rather than green, revealing an attribute error. In this setting, the incorrect attribute naturally yields a targeted negative prompt

(“yellow fire hydrant”), while an untargeted negative is chosen from incidental attributes present in the image but irrelevant to the error (e.g., “vintage television”).

The BASE model attains a salient-attention score of 0.069, which increases to 0.096 with targeted negative guidance (39.13%) and to 0.075 with an untargeted negative (8.70%). Rather than merely correcting the hydrant’s appearance, these changes reflect how negative prompting reshapes the model’s internal focus: the targeted negative suppresses the erroneous attribute, enabling attention to shift back toward the intended “green,” while the untargeted negative reduces emphasis on unrelated background elements. Together, these results show that negative prompts—whether directly or indirectly related to the misalignment—can reallocate attention toward the prompt’s salient components and thereby improve alignment. Although both types of negatives help, their effectiveness varies across prompt–image pairs (p, x) , making manual selection difficult and motivating an automated mechanism.

4. NPC

In this section, we introduce NPC, an automated pipeline for selecting effective negative prompts by (i) generating

candidates (Section 4.1) and (ii) scoring them with a salient text-space measure that requires no additional image generation (Section 4.2). Figure 3 provides an overview.

4.1. Negative Prompt Candidate Generation

As the efficacy of negative prompts is unknown *a priori*, it is natural to generate a set of candidates. To cover the full design space—including both *targeted* and *untargeted* negatives—we employ distinct agents with complementary roles. Given an positive prompt p and its generated image x_p , NPC uses three agents—the *verifier*, *captioner*, and *proposer*—to produce negative–prompt candidates. A concise version of the LLM prompts that define each agent’s role is shown in Figure 4.

- **Verifier** V checks whether x_p satisfies alignment criteria w.r.t. p and returns $(\text{correct}, s_V, r)$, where $\text{correct} \in \{0, 1\}$, $s_V \in [0, 1]$ is a confidence score, and r is a short reason string (e.g., missing attributes, wrong style, prohibited content) that can serve as *targeted* negatives.
- **Captioner** C produces a descriptive caption c_x of x_p , enumerating incidental objects, attributes, and context to supply *untargeted* negatives.
- **Proposer** P distills r and c_x into concise (typically one- or two-token) negative prompts. Conditioning on (p, r, c_x) , it proposes $K \in \mathbb{N}$ candidates $\mathcal{N} = \{n_1, \dots, n_K\}$. Each n_k is either *targeted*—directly addressing r —or *untargeted*—suppressing incidental scene elements hypothesized to interfere with alignment.

Pipeline We first generate x_p and query $V(x_p, p)$. If $\text{correct} = 1$, we skip NPC and return x_p as is (pre-check in Figure 3). Otherwise, we obtain $r \leftarrow V(x_p, p)$ and $c_x \leftarrow C(x_p)$, then form $\mathcal{N} \leftarrow P(p, r, c_x)$. Section 4.2 details *automated effective negative prompt selection*, in which candidates in \mathcal{N} are *scored in text space* (without additional image synthesis) and the top-scoring prompt is selected.

4.2. Negative Prompt Selection

To minimize re-generation trials without incurring additional compute or latency, NPC introduces a proxy *text-space* scorer—the *salient score*—which estimates how a negative prompt n will affect alignment with the salient content of the positive prompt p using only the model’s text encoder. Intuitively, the score (i) models how adding n shifts the text embedding of p , (ii) identifies salient tokens in p (e.g., key objects or attributes), and (iii) measures how well this shift aligns with those salient tokens via cosine similarity. Averaging these similarities yields a scalar score that ranks negative candidates without requiring any image synthesis. Although this text-space measure is not an

Verifier

<System Prompt>: You are an image evaluator. Judge if an image satisfies a given instruction. Apply strict rules: all conditions must hold; reject unrealistic or stylized images. Return only a JSON object with fields: $\{\text{"correct": 1 or 0, "score": [0-1], "reason": \text{"short explanation"}\}$

<User Prompt>: **POSITIVE PROMPT:** \$positive_prompt Evaluate the attached image and return the JSON result.

Captioner

<System Prompt>: You are a visual describer. Generate a detailed, factual caption of the given image. Include objects, attributes, spatial relations, background, lighting, and style. Avoid speculation or subjective impressions. Output plain text only.

<User Prompt>: Describe this image.

Proposer

<System Prompt>: You are a prompt editor. Given a positive prompt and an image caption, generate concise negative prompt candidates that suppress undesired or contradictory elements. Output only a JSON object: $\{\text{"candidates": ["...", "...", "..."]}\}$

<User Prompt>: **POSITIVE PROMPT:** \$positive_prompt **CAPTION:** \$caption **FAILURE REASON:** \$reason **K:** \$k Return up to K concise negative phrases that are inconsistent with the positive prompt, or directly address the failure reason.

Figure 4. Summarized LLM prompts for each agent (see Section F for full versions). Inputs are shown in bold in the user prompt, while outputs are underlined in the system prompt.

exact proxy for image-level effects, it is effective for comparative evaluation and candidate selection; see Section 5.3 for empirical evidence.

Formally, let $\mathbf{E}(\cdot) \in \mathbb{R}^{L \times d}$ denote token-level outputs of the text encoder [52], and let $\text{pool}(\cdot)$ be a fixed pooling operator (mean over tokens). We form pooled embeddings $\bar{\mathbf{e}}_p = \text{pool}(\mathbf{E}(p))$ and $\bar{\mathbf{e}}_n = \text{pool}(\mathbf{E}(n))$, and use cosine similarity $\cos(\mathbf{a}, \mathbf{b}) = \langle \mathbf{a}, \mathbf{b} \rangle / (\|\mathbf{a}\| \|\mathbf{b}\|)$. The *direction of change* induced by adding n is modeled as the subtractive direction $\mathbf{d}(p, n) = \bar{\mathbf{e}}_p - \bar{\mathbf{e}}_n$, treating n as pulling the representation away from content associated with n .

We extract *salient tokens* from a prompt using a simple heuristic: we identify *quantity tokens* (e.g., “a”, “two”) and take the noun that immediately follows each quantity token as a salient-token candidate. For example, for the prompt “A jelly-like dolphin and a steel-reinforced dam coexist in

Method	Color	Count	Color/Count	Color/Pos	Pos/Count	Pos/Size	Multi-Count	Overall
SDv2.1 [54]	0.000	0.325	0.025	0.000	0.000	0.025	0.075	0.064
SDXL [49]	0.050	0.375	0.000	0.000	0.000	0.000	0.000	0.061
SDv3-medium [11]	<u>0.550</u>	0.500	0.125	0.350	0.175	0.150	0.225	0.296
FLUX.1-Kontext [27]	0.425	0.500	0.200	0.250	<u>0.300</u>	0.400	0.325	0.343
FLUX.1-dev [26]	0.350	<u>0.625</u>	0.150	0.275	0.200	0.375	0.225	0.314
Janus-Pro [7]	0.450	0.300	0.125	0.300	0.075	0.350	0.125	0.246
T2I-R1 [24]	0.675	0.325	0.200	0.350	0.075	0.250	0.300	0.311
BLIP3-o 4B [6]	0.125	0.225	0.100	0.450	0.125	0.550	0.225	0.257
BLIP3-o 8B [6]	0.250	0.250	0.125	0.600	0.125	<u>0.575</u>	0.225	0.307
OmniGen2 [65]	<u>0.550</u>	0.425	0.200	0.275	0.125	0.250	<u>0.450</u>	0.325
Bagel [10]	0.325	0.600	<u>0.250</u>	0.325	0.250	0.475	0.375	<u>0.371</u>
NPC (Ours)	<u>0.550</u>	0.675	0.350	<u>0.525</u>	0.550	0.725	0.625	0.571

Table 1. Comparative results on GenEval++ assessing diverse compositional generation capability. Each sample is scored 0/1 based on correctness, so the reported values are accuracies. Bold indicates the best result, and underlined denotes the second best (ties underlined).

Method	Attribute shift	Spatiotemporal	Hybridization	Multi-Object	Overall
SDv2.1 [54]	4.46	5.06	4.12	3.49	4.30
SDXL [49]	4.42	6.32	4.93	4.50	4.97
SDv3-medium [11]	5.14	5.91	6.30	6.07	5.78
FLUX.1-Kontext [27]	5.33	6.49	5.48	5.34	5.62
FLUX.1-dev [26]	5.68	7.13	6.38	5.24	6.06
Janus-Pro [7]	5.30	7.28	6.73	6.04	6.22
T2I-R1 [24]	<u>5.85</u>	7.70	<u>7.36</u>	6.68	<u>6.78</u>
BLIP3-o 4B [6]	5.48	6.79	6.93	6.09	6.23
BLIP3-o 8B [6]	5.80	7.08	7.06	6.44	6.51
OmniGen2 [65]	5.28	<u>7.45</u>	6.29	6.31	6.22
Bagel [10]	5.37	6.93	6.50	6.41	6.20
NPC (Ours)	6.31	6.76	7.57	<u>6.52</u>	6.80

Table 2. Comparative results on Imagine-Bench assessing the ability to generate surreal modifications. A detailed description of the scoring is provided in Section 5.1. Bold indicates the best result; underlined denotes the second best.

the gentle riverbed flow,” our procedure yields $\mathcal{S}_{\text{sal}}(p) = \{\text{jelly-like, steel-reinforced}\}$. For each $t \in \mathcal{S}_{\text{sal}}(p)$, define $\mathbf{v}_t = \text{pool}(\mathbf{E}(t))$ and $s_t = \cos(\mathbf{d}(p, n), \mathbf{v}_t)$. The *salient score* is then

$$s_{\text{sal}}(p, n) \triangleq \frac{1}{|\mathcal{S}_{\text{sal}}(p)|} \sum_{t \in \mathcal{S}_{\text{sal}}(p)} s_t.$$

A higher $s_{\text{sal}}(p, n)$ indicates that $\mathbf{d}(p, n)$ is better aligned with the salient content of p —i.e., the negative tends to preserve core semantics and is more likely to be alignment-preserving. Accordingly, we process candidates in decreasing order of $s_{\text{sal}}(p, n)$ and synthesize images following this order (with early stopping once alignment is satisfied).

Stopping rule Given candidates $\{n_i\}_{i=1}^K$ (in the prescribed order), for $i = 1, \dots, K$ generate x_{p, n_i} under

(p, n_i) and query $V(x_{p, n_i}, p)$. Terminate at the first i with $\text{correct} = 1$ and output x_i . If no such i exists, fallback to the image with the highest verifier score s_{V_i} , i.e., output $x_{p, n_{i^*}}$ where $i^* = \arg \max_i s_{V_i}$.

5. Experiments

5.1. Experimental Setting

Implementation details We instantiate the image generator with FLUX.1-dev [26]. The *Captioner* and the *Proposer* are implemented with GPT-4o-mini [44], and the *Verifier* uses GPT-4.1 [43]. Additional experiments using other image generators and alternative MLLM or LLM configurations can be found in Section D. For each prompt p , the *Proposer* returns $K = 5$ candidates $\mathcal{N} = \{n_1, \dots, n_5\}$. Diffusion sampling uses $T = 50$ denoising steps; to reduce

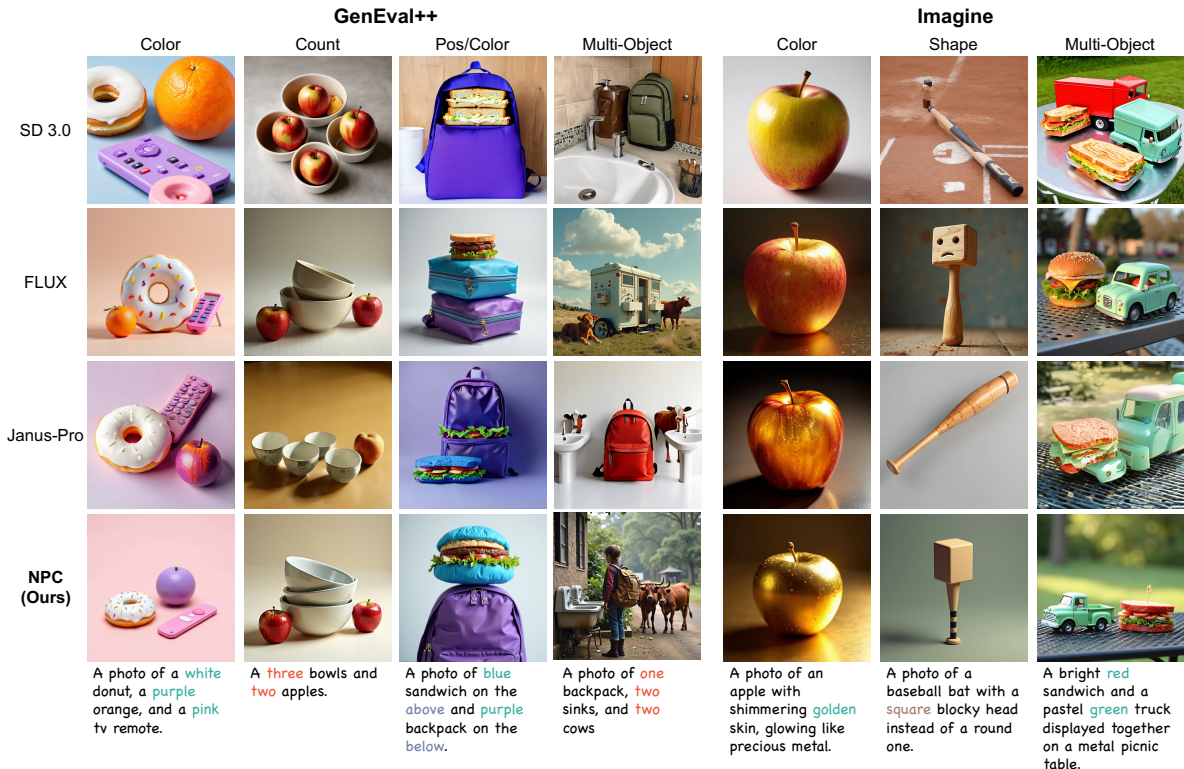


Figure 5. Qualitative comparison on GenEval++ and Imagine-Bench: NPC (samples generated with FLUX) consistently achieves alignment across diverse tasks, while other methods fail in some cases.

computation, we apply the negative prompt only in the first three ($t = 1, 2, 3$), as later steps are empirically observed to have negligible influence. Unless otherwise noted, we set the guidance scale to 3.5 and the true-CFG scale (a variant of classifier-free guidance that uses the direct difference between conditional and unconditional prediction) to 1.8.

Datasets and evaluation We evaluate two benchmarks, recently proposed by [75], that assess instruction fidelity and creative synthesis.

GenEval++ This benchmark provides 280 prompts (seven task types with 40 prompts each) featuring richer semantics and more diverse compositions than prior instruction-following sets. A GPT-4.1 [43] multimodal evaluator assesses image-text consistency using a fixed checklist over *Object*, *Counts*, *Color*, *Position*, and *Size*; a result is marked correct only if all criteria are satisfied. To match the “A photo of ...” prompt style, anime-style renderings and images with multiple disjoint elements are deemed invalid.

Imagine-Bench This benchmark contains 270 creative instructions that modify common objects with fantastical attributes while preserving identity. For each instruction, GPT-4o [44] produces a checklist specifying the required fantastical modifications and the object’s invariant

identity cues. Given the prompt and image, GPT-4.1 assigns 0–10 scores on three dimensions—*Fantasy Fulfillment*, *Identity Preservation*, and *Aesthetic Quality*—with explicit rationales. The final score is computed as $0.8 \times \min(\text{Fantasy Fulfillment}, \text{Identity Preservation}) + 0.2 \times \text{Aesthetic Quality}$. Additional text-image alignment benchmark results—DPG-Bench [18], and T2I-CompBench [20]—are in Section A.

Baselines We compare NPC against four groups, all of which are strong baselines: (i) **Stable Diffusion series**—SD v2.1 [54], SDXL [49], and SD3-Medium [11]—strong open T2I diffusion baselines; (ii) **FLUX.1 family**—FLUX.1-dev [26] and FLUX.1-Kontext [27]—rectified-flow Transformer T2I models, with *Kontext* enabling in-context conditioning/editing; (iii) **Unified multimodal generators**—BLIP3-o (4B/8B) [6], OmniGen2 [65], and Bagel [10]—models trained for joint understanding and generation via large-scale pretraining; and (iv) **Reasoning/AR frameworks**—Janus-Pro [7] and T2I-R1 [24]—autoregressive or unified approaches that incorporate chain-of-thought or RL signals to enhance instruction following. Additional comparison results against other text-image alignment baselines are provided in Section A.

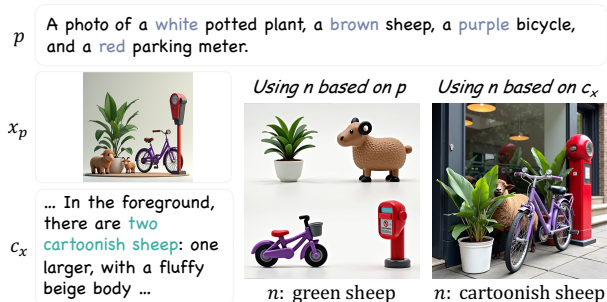


Figure 6. Ablation of negative-prompt generation (Section 5.3): negatives generated from the original prompt (p) vs. those generated from the original prompt with the caption additionally provided (NPC). NPC yields the more realistic result.

5.2. Main Results

Table 1 and Table 2 collectively demonstrate that NPC attains state-of-the-art performance across both benchmarks. On GenEval++ (Table 1), NPC achieves the highest overall score (0.571), surpassing the strongest unified baseline, Bagel (0.371), with pronounced gains on positional/compositional constraints—Count/Pos, Pos/Size, and Multi-Count. For Color and Color/Pos, NPC ranks second best—narrowly trailing the strongest baselines—reflecting competitive, near-leading performance in these dimensions. On Imagine-Bench (Table 2), NPC achieves the best overall score (6.80) and ranks first in all categories except *Spatiotemporal*, where T2I-R1 leads. Overall, these results indicate that NPC performs robustly across diverse task types on Imagine-Bench; qualitative comparisons with recent T2I models are shown in Figure 5.

5.3. Ablation Study

This section presents ablations of the two core components of NPC: (i) negative-prompt candidate generation and (ii) selection based on a salient text-space metric. We evaluate each component on GenEval++ and quantify its impact on alignment quality and computational efficiency.

Negative Prompt Generation To incorporate information from the original image, we condition the *proposer* on a **caption** when generating negatives. For validation, we compare NPC (caption-conditioned) with a prompt-only baseline that proposes negatives from the original prompt using a separate *proposer* (LLM instructions in Table S11). NPC marginally but consistently outperforms the prompt-only baseline on GenEval++—0.57 vs. 0.53 accuracy—indicating that grounding negatives in actual image content is more effective. This ablation is designed to assess the utility of the *captioner*; consistent with the quantitative result, Figure 6 shows that grounded negatives (e.g., “cartoonish sheep”) produce more realistic outputs than nega-

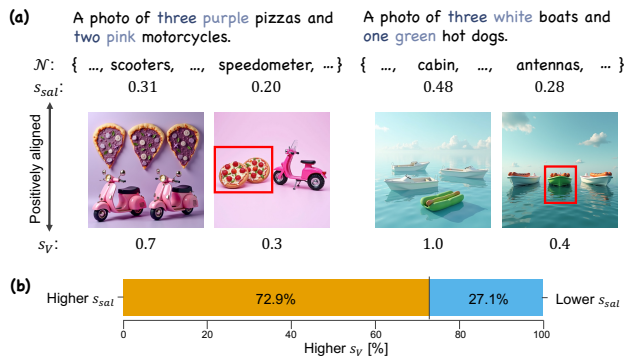


Figure 7. Examples of relationship between salient score (s_{sal}) and verifier score (s_V) (Section 5.3); the higher-salient negative yields the higher verifier score.

tives targeting attributes not supported by the image (e.g., “green sheep”).

Salient Score To assess how useful the salient score is as a priority signal for the selection step of NPC, we run two tests: (1) **regeneration efficiency**—holding the candidate set fixed (with five candidates), we compare descending salient-score order against a random order; random ordering can push an effective negative to the back, increasing total generations, whereas prioritization lowers the mean number of attempts from 4.1 to 2.5; and (2) **alignment quality**—for each prompt, we choose two negatives with different priorities, generate one image per negative under identical conditions, and compare verifier scores; the higher-salience negative attains the higher verifier score in 204/280 pairs (72.9%; examples in Figure 7). These results indicate that the salient score provides an effective and practical priority signal for negative prompt selection, both reducing regeneration and improving alignment quality.

6. Conclusion

We propose NPC, an automated pipeline that improves text-to-image alignment by discovering and selecting *effective negative prompts*. Beyond resolving explicit prompt conflicts, our image-text attention analysis shows that *untargeted* negatives—derived from incidental visual attributes—also strengthen alignment. NPC consists of (i) a verifier-captioner-proposer framework that generates both targeted and untargeted negatives, and (ii) a selection stage that ranks candidates with a salient text-space metric to minimize regeneration. In experiments, NPC yields strong alignment gains with modest generation overhead. These results highlight the central role of negative-prompt design in accurate, reliable image generation and point to promising directions for further progress.

Acknowledgements

This work was supported by the National Research Foundation of Korea (NRF) grant funded by the Korea government (MSIT) [No. 2022R1A3B1077720; 2022R1A5A708390811], Institute of Information & Communications Technology Planning & Evaluation (IITP) grant funded by the Korea government (MSIT) [RS-2022-II220959; No.RS-2021-II211343, Artificial Intelligence Graduate School Program (Seoul National University)], the BK21 FOUR program of the Education and Research Program for Future ICT Pioneers, Seoul National University in 2025. This research was also conducted as part of the Sovereign AI Foundation Model Project (Data Track), organized by MSIT and supported by the National Information Society Agency (NIA) of Korea [No.2025-AI Data-wi43].

References

- [1] Josh Achiam, Steven Adler, Sandhini Agarwal, Lama Ahmad, Ilge Akkaya, Florencia Leoni Aleman, Diogo Almeida, Janko Altenschmidt, Sam Altman, Shyamal Anadkat, et al. Gpt-4 technical report. *arXiv preprint arXiv:2303.08774*, 2023. 2
- [2] Shuai Bai, Keqin Chen, Xuejing Liu, Jialin Wang, Wenbin Ge, Sibao Song, Kai Dang, Peng Wang, Shijie Wang, Jun Tang, et al. Qwen2. 5-vl technical report. *arXiv preprint arXiv:2502.13923*, 2025. 2
- [3] James Betker, Gabriel Goh, Li Jing, Tim Brooks, Jianfeng Wang, Linjie Li, Long Ouyang, Juntang Zhuang, Joyce Lee, Yufei Guo, et al. Improving image generation with better captions. *Computer Science*. <https://cdn.openai.com/papers/dall-e-3.pdf>, 2(3):8, 2023. 1, 2, 4
- [4] Hila Chefer, Yuval Alaluf, Yael Vinker, Lior Wolf, and Daniel Cohen-Or. Attend-and-excite: Attention-based semantic guidance for text-to-image diffusion models. *ACM Transactions on Graphics (TOG)*, 42(4):1–10, 2023. 2, 1
- [5] Chieh-Yun Chen, Min Shi, Gong Zhang, and Humphrey Shi. T2i-copilot: A training-free multi-agent text-to-image system for enhanced prompt interpretation and interactive generation. *arXiv preprint arXiv:2507.20536*, 2025. 1, 3
- [6] Jiuhai Chen, Zhiyang Xu, Xichen Pan, Yushi Hu, Can Qin, Tom Goldstein, Lifu Huang, Tianyi Zhou, Saining Xie, Silvio Savarese, et al. Blip3-o: A family of fully open unified multimodal models-architecture, training and dataset. *arXiv preprint arXiv:2505.09568*, 2025. 2, 6, 7
- [7] Xiaokang Chen, Zhiyu Wu, Xingchao Liu, Zizheng Pan, Wen Liu, Zhenda Xie, Xingkai Yu, and Chong Ruan. Januspro: Unified multimodal understanding and generation with data and model scaling. *arXiv preprint arXiv:2501.17811*, 2025. 2, 6, 7, 4
- [8] Jaemin Cho, Yushi Hu, Jason Michael Baldrige, Roopal Garg, Peter Anderson, Ranjay Krishna, Mohit Bansal, Jordi Pont-Tuset, and Su Wang. Davidsonian scene graph: Improving reliability in fine-grained evaluation for text-to-image generation. In *The Twelfth International Conference on Learning Representations*. 2
- [9] Hyung Won Chung, Le Hou, Shayne Longpre, Barret Zoph, Yi Tay, William Fedus, Yunxuan Li, Xuezhi Wang, Mostafa Dehghani, Siddhartha Brahma, et al. Scaling instruction-finetuned language models. *Journal of Machine Learning Research*, 25(70):1–53, 2024. 2
- [10] Chaorui Deng, Deyao Zhu, Kunchang Li, Chenhui Gou, Feng Li, Zeyu Wang, Shu Zhong, Weihao Yu, Xiaonan Nie, Ziang Song, et al. Emerging properties in unified multimodal pretraining. *arXiv preprint arXiv:2505.14683*, 2025. 2, 6, 7, 4
- [11] Patrick Esser, Sumith Kulal, Andreas Blattmann, Rahim Entezari, Jonas Müller, Harry Saini, Yam Levi, Dominik Lorenz, Axel Sauer, Frederic Boesel, et al. Scaling rectified flow transformers for high-resolution image synthesis. In *Forty-first International Conference on Machine Learning*, 2024. 1, 2, 3, 6, 7, 4, 5
- [12] Brian Gordon, Yonatan Bitton, Yonatan Shafir, Roopal Garg, Xi Chen, Dani Lischinski, Daniel Cohen-Or, and Idan Szepesktor. Mismatch quest: Visual and textual feedback for image-text misalignment. In *European Conference on Computer Vision*, pages 310–328. Springer, 2025. 2
- [13] Xiefan Guo, Jinlin Liu, Miaomiao Cui, Jiankai Li, Hongyu Yang, and Di Huang. Initno: Boosting text-to-image diffusion models via initial noise optimization. In *Proceedings of the IEEE/CVF Conference on Computer Vision and Pattern Recognition*, pages 9380–9389, 2024. 2
- [14] Yaru Hao, Zewen Chi, Li Dong, and Furu Wei. Optimizing prompts for text-to-image generation. In *Thirty-seventh Conference on Neural Information Processing Systems*, 2023. 2
- [15] Jack Hessel, Ari Holtzman, Maxwell Forbes, Ronan Le Bras, and Yejin Choi. Clipscore: A reference-free evaluation metric for image captioning. In *Proceedings of the 2021 Conference on Empirical Methods in Natural Language Processing*, pages 7514–7528, 2021. 1
- [16] Jonathan Ho and Tim Salimans. Classifier-free diffusion guidance. In *NeurIPS 2021 Workshop on Deep Generative Models and Downstream Applications*, 2021. 2
- [17] Jonathan Ho, Ajay Jain, and Pieter Abbeel. Denoising diffusion probabilistic models. *Advances in neural information processing systems*, 33:6840–6851, 2020. 2
- [18] Xiwei Hu, Rui Wang, Yixiao Fang, Bin Fu, Pei Cheng, and Gang Yu. Ella: Equip diffusion models with llm for enhanced semantic alignment. *arXiv e-prints*, pages arXiv-2403, 2024. 1, 7
- [19] Yushi Hu, Benlin Liu, Jungo Kasai, Yizhong Wang, Mari Ostendorf, Ranjay Krishna, and Noah A Smith. Tifa: Accurate and interpretable text-to-image faithfulness evaluation with question answering. In *Proceedings of the IEEE/CVF International Conference on Computer Vision*, pages 20406–20417, 2023. 2
- [20] Kaiyi Huang, Kaiyue Sun, Enze Xie, Zhenguo Li, and Xihui Liu. T2i-compbench: A comprehensive benchmark for open-world compositional text-to-image generation. *Advances in Neural Information Processing Systems*, 36:78723–78747, 2023. 2, 7, 1
- [21] Saar Huberman, Or Patashnik, Omer Dahary, Ron Mokady, and Daniel Cohen-Or. Image generation from contextually-

- contradictory prompts. *arXiv preprint arXiv:2506.01929*, 2025. 1
- [22] Aaron Hurst, Adam Lerer, Adam P Goucher, Adam Perelman, Aditya Ramesh, Aidan Clark, AJ Ostrow, Akila Welihinda, Alan Hayes, Alec Radford, et al. Gpt-4o system card. *arXiv preprint arXiv:2410.21276*, 2024. 1
- [23] Dongzhi Jiang, Guanglu Song, Xiaoshi Wu, Renrui Zhang, Dazhong Shen, Zhuofan Zong, Yu Liu, and Hongsheng Li. Comat: Aligning text-to-image diffusion model with image-to-text concept matching. *arXiv preprint arXiv:2404.03653*, 2024. 2, 1
- [24] Dongzhi Jiang, Ziyu Guo, Renrui Zhang, Zhuofan Zong, Hao Li, Le Zhuo, Shilin Yan, Pheng-Ann Heng, and Hongsheng Li. T2i-r1: Reinforcing image generation with collaborative semantic-level and token-level cot. *arXiv preprint arXiv:2505.00703*, 2025. 6, 7, 4
- [25] Mohammed Abdul Hafeez Khan, Yash Jain, Siddhartha Bhattacharyya, and Vibhav Vineet. Test-time prompt refinement for text-to-image models. In *Proceedings of the IEEE/CVF International Conference on Computer Vision*, pages 6506–6516, 2025. 3
- [26] Black Forest Labs. Black Forest Labs; Frontier AI Lab. 1, 6, 7, 4, 5
- [27] Black Forest Labs, Stephen Batifol, Andreas Blattmann, Frederic Boesel, Saksham Consul, Cyril Diagne, Tim Dockhorn, Jack English, Zion English, Patrick Esser, et al. Flux. 1 kontext: Flow matching for in-context image generation and editing in latent space. *arXiv preprint arXiv:2506.15742*, 2025. 3, 6, 7
- [28] Baiqi Li, Zhiqiu Lin, Deepak Pathak, Jiayao Li, Yixin Fei, Kewen Wu, Tiffany Ling, Xide Xia, Pengchuan Zhang, Graham Neubig, et al. Genai-bench: Evaluating and improving compositional text-to-visual generation. *arXiv preprint arXiv:2406.13743*, 2024. 1
- [29] Chenliang Li, Haiyang Xu, Junfeng Tian, Wei Wang, Ming Yan, Bin Bi, Jiabo Ye, He Chen, Guohai Xu, Zheng Cao, Ji Zhang, Songfang Huang, Fei Huang, Jingren Zhou, and Luo Si. mPLUG: Effective and efficient vision-language learning by cross-modal skip-connections. In *Proceedings of the 2022 Conference on Empirical Methods in Natural Language Processing*, pages 7241–7259, Abu Dhabi, United Arab Emirates, 2022. Association for Computational Linguistics. 1
- [30] Yuheng Li, Haotian Liu, Qingyang Wu, Fangzhou Mu, Jianwei Yang, Jianfeng Gao, Chunyuan Li, and Yong Jae Lee. Gligen: Open-set grounded text-to-image generation. In *Proceedings of the IEEE/CVF Conference on Computer Vision and Pattern Recognition*, pages 22511–22521, 2023. 2
- [31] Zhimin Li, Jianwei Zhang, Qin Lin, Jiangfeng Xiong, Yanxin Long, Xincheng Deng, Yingfang Zhang, Xingchao Liu, Minbin Huang, Zedong Xiao, et al. Hunyuan-dit: A powerful multi-resolution diffusion transformer with fine-grained chinese understanding. *arXiv preprint arXiv:2405.08748*, 2024. 4
- [32] Long Lian, Boyi Li, Adam Yala, and Trevor Darrell. LLM-grounded diffusion: Enhancing prompt understanding of text-to-image diffusion models with large language models. *Transactions on Machine Learning Research*, 2024. Featured Certification. 1, 2, 3
- [33] Youwei Liang, Junfeng He, Gang Li, Peizhao Li, Arseniy Klimovskiy, Nicholas Carolan, Jiao Sun, Jordi Pont-Tuset, Sarah Young, Feng Yang, et al. Rich human feedback for text-to-image generation. In *Proceedings of the IEEE/CVF Conference on Computer Vision and Pattern Recognition*, pages 19401–19411, 2024. 2
- [34] Bin Lin, Zongjian Li, Xinhua Cheng, Yuwei Niu, Yang Ye, Xianyi He, Shenghai Yuan, Wangbo Yu, Shaodong Wang, Yunyang Ge, et al. Uniworld: High-resolution semantic encoders for unified visual understanding and generation. *arXiv preprint arXiv:2506.03147*, 2025. 4
- [35] Zhiqiu Lin, Deepak Pathak, Baiqi Li, Jiayao Li, Xide Xia, Graham Neubig, Pengchuan Zhang, and Deva Ramanan. Evaluating text-to-visual generation with image-to-text generation. In *European Conference on Computer Vision*, pages 366–384. Springer, 2025. 2
- [36] Yaron Lipman, Ricky TQ Chen, Heli Ben-Hamu, Maximilian Nickel, and Matthew Le. Flow matching for generative modeling. In *The Eleventh International Conference on Learning Representations*, 2023. 3
- [37] Nan Liu, Shuang Li, Yilun Du, Antonio Torralba, and Joshua B Tenenbaum. Compositional visual generation with composable diffusion models. In *European Conference on Computer Vision*, pages 423–439. Springer, 2022. 2
- [38] Xingchao Liu, Chengyue Gong, et al. Flow straight and fast: Learning to generate and transfer data with rectified flow. In *The Eleventh International Conference on Learning Representations*, 2023. 3
- [39] Yujie Lu, Xianjun Yang, Xiujun Li, Xin Eric Wang, and William Yang Wang. Llm-score: Unveiling the power of large language models in text-to-image synthesis evaluation. *Advances in Neural Information Processing Systems*, 36, 2024. 2
- [40] Wenyi Mo, Tianyu Zhang, Yalong Bai, Bing Su, Ji-Rong Wen, and Qing Yang. Dynamic prompt optimizing for text-to-image generation. In *Proceedings of the IEEE/CVF Conference on Computer Vision and Pattern Recognition (CVPR)*, pages 26627–26636, 2024. 2
- [41] Ofir Nabati, Guy Tennenholtz, ChihWei Hsu, Moonkyung Ryu, Deepak Ramachandran, Yinlam Chow, Xiang Li, and Craig Boutilier. Personalized and sequential text-to-image generation. *arXiv e-prints*, pages arXiv–2412, 2024. 3
- [42] Alex Nichol, Prafulla Dhariwal, Aditya Ramesh, Pranav Shyam, Pamela Mishkin, Bob McGrew, Ilya Sutskever, and Mark Chen. Glide: Towards photorealistic image generation and editing with text-guided diffusion models. *arXiv preprint arXiv:2112.10741*, 2021. 2
- [43] OpenAI. Gpt-4.1. <https://openai.com/index/gpt-4-1>, 2025. 6, 7
- [44] OpenAI. Gpt-4o. <https://openai.com/index/introducing-4o-image-generation>, 2025. 6, 7
- [45] Dongmin Park, Sebin Kim, Taehong Moon, Minkyu Kim, Kangwook Lee, and Jaewoong Cho. Rare-to-frequent: Unlocking compositional generation power of diffusion models on rare concepts with llm guidance. *arXiv preprint arXiv:2410.22376*, 2024. 1

- [46] Dongmin Park, Sebin Kim, Taehong Moon, Minkyu Kim, Kangwook Lee, and Jaewoong Cho. Rare-to-frequent: Unlocking compositional generation power of diffusion models on rare concepts with LLM guidance. In *The Thirteenth International Conference on Learning Representations*, 2025. 1
- [47] William Peebles and Saining Xie. Scalable diffusion models with transformers. In *Proceedings of the IEEE/CVF International Conference on Computer Vision*, pages 4195–4205, 2023. 3
- [48] William Peebles and Saining Xie. Scalable diffusion models with transformers. In *Proceedings of the IEEE/CVF international conference on computer vision*, pages 4195–4205, 2023. 1
- [49] Dustin Podell, Zion English, Kyle Lacey, Andreas Blattmann, Tim Dockhorn, Jonas Müller, Joe Penna, and Robin Rombach. Sdxl: Improving latent diffusion models for high-resolution image synthesis. In *The Twelfth International Conference on Learning Representations*. 1, 3, 6, 7, 4, 5
- [50] Liao Qu, Huichao Zhang, Yiheng Liu, Xu Wang, Yi Jiang, Yiming Gao, Hu Ye, Daniel K Du, Zehuan Yuan, and Xinglong Wu. Tokenflow: Unified image tokenizer for multi-modal understanding and generation. In *Proceedings of the Computer Vision and Pattern Recognition Conference*, pages 2545–2555, 2025. 4
- [51] Alec Radford, Jong Wook Kim, Chris Hallacy, Aditya Ramesh, Gabriel Goh, Sandhini Agarwal, Girish Sastry, Amanda Askell, Pamela Mishkin, Jack Clark, et al. Learning transferable visual models from natural language supervision. In *International conference on machine learning*, pages 8748–8763. PMLR, 2021. 2, 1
- [52] Colin Raffel, Noam Shazeer, Adam Roberts, Katherine Lee, Sharan Narang, Michael Matena, Yanqi Zhou, Wei Li, and Peter J Liu. Exploring the limits of transfer learning with a unified text-to-text transformer. *Journal of machine learning research*, 21(140):1–67, 2020. 5
- [53] Royi Rassin, Eran Hirsch, Daniel Glickman, Shauli Ravfogel, Yoav Goldberg, and Gal Chechik. Linguistic binding in diffusion models: Enhancing attribute correspondence through attention map alignment. *Advances in Neural Information Processing Systems*, 36, 2024. 2, 1, 3
- [54] Robin Rombach, Andreas Blattmann, Dominik Lorenz, Patrick Esser, and Björn Ommer. High-resolution image synthesis with latent diffusion models. In *Proceedings of the IEEE/CVF conference on computer vision and pattern recognition*, pages 10684–10695, 2022. 1, 2, 3, 6, 7
- [55] Chitwan Saharia, William Chan, Saurabh Saxena, Lala Li, Jay Whang, Emily L Denton, Kamyar Ghasemipour, Raphael Gontijo Lopes, Burcu Karagol Ayan, Tim Salimans, et al. Photorealistic text-to-image diffusion models with deep language understanding. *Advances in neural information processing systems*, 35:36479–36494, 2022. 2
- [56] Jaskirat Singh and Liang Zheng. Divide, evaluate, and refine: Evaluating and improving text-to-image alignment with iterative vqa feedback. *Advances in Neural Information Processing Systems*, 36:70799–70811, 2023. 2
- [57] Jascha Sohl-Dickstein, Eric Weiss, Niru Maheswaranathan, and Surya Ganguli. Deep unsupervised learning using nonequilibrium thermodynamics. In *International conference on machine learning*, pages 2256–2265. PMLR, 2015. 2
- [58] Xingchen Wan, Han Zhou, Ruoxi Sun, Hootan Nakhost, Ke Jiang, Rajarishi Sinha, and Sercan Ö Arık. Maestro: Self-improving text-to-image generation via agent orchestration. *arXiv preprint arXiv:2509.10704*, 2025. 3
- [59] Linqing Wang, Ximing Xing, Yiji Cheng, Zhiyuan Zhao, Jiale Tao, Qixun Wang, Ruihuang Li, Xin Li, Mingrui Wu, Xincheng Deng, et al. Promptenhancer: A simple approach to enhance text-to-image models via chain-of-thought prompt rewriting. *arXiv preprint arXiv:2509.04545*, 2025. 1
- [60] Ruochen Wang, Ting Liu, Cho-Jui Hsieh, and Boqing Gong. On discrete prompt optimization for diffusion models. In *Proceedings of the 41st International Conference on Machine Learning*, pages 50992–51011. PMLR, 2024. 2
- [61] Xudong Wang, Trevor Darrell, Sai Saketh Rambhatla, Rohit Girdhar, and Ishan Misra. Instancediffusion: Instance-level control for image generation. In *Proceedings of the IEEE/CVF Conference on Computer Vision and Pattern Recognition*, pages 6232–6242, 2024. 2, 1
- [62] Xinlong Wang, Xiaosong Zhang, Zhengxiong Luo, Quan Sun, Yufeng Cui, Jinsheng Wang, Fan Zhang, Yueze Wang, Zhen Li, Qiyang Yu, et al. Emu3: Next-token prediction is all you need. *arXiv preprint arXiv:2409.18869*, 2024. 4
- [63] Zirui Wang, Zhizhou Sha, Zheng Ding, Yilin Wang, and Zhuowen Tu. Tokencompose: Grounding diffusion with token-level supervision. *arXiv preprint arXiv:2312.03626*, 2023. 2
- [64] Zhenyu Wang, Aoxue Li, Zhenguo Li, and Xihui Liu. Genartist: Multimodal llm as an agent for unified image generation and editing. *Advances in Neural Information Processing Systems*, 37:128374–128395, 2024. 3
- [65] Chenyuan Wu, Pengfei Zheng, Ruiran Yan, Shitao Xiao, Xin Luo, Yueze Wang, Wanli Li, Xiyang Jiang, Yexin Liu, Junjie Zhou, et al. Omnigen2: Exploration to advanced multimodal generation. *arXiv preprint arXiv:2506.18871*, 2025. 2, 6, 7, 4
- [66] Tsung-Han Wu, Long Lian, Joseph E Gonzalez, Boyi Li, and Trevor Darrell. Self-correcting llm-controlled diffusion models. In *Proceedings of the IEEE/CVF Conference on Computer Vision and Pattern Recognition*, pages 6327–6336, 2024. 1, 3
- [67] Xiaoshi Wu, Keqiang Sun, Feng Zhu, Rui Zhao, and Hongsheng Li. Human preference score: Better aligning text-to-image models with human preference. In *Proceedings of the IEEE/CVF International Conference on Computer Vision*, pages 2096–2105, 2023. 2
- [68] Shitao Xiao, Yueze Wang, Junjie Zhou, Huaying Yuan, Xingrun Xing, Ruiran Yan, Chaofan Li, Shuting Wang, Tiejun Huang, and Zheng Liu. Omnigen: Unified image generation. In *Proceedings of the Computer Vision and Pattern Recognition Conference*, pages 13294–13304, 2025. 4
- [69] Jinheng Xie, Yuexiang Li, Yawen Huang, Haozhe Liu, Wentian Zhang, Yefeng Zheng, and Mike Zheng Shou. Boxdiff:

- Text-to-image synthesis with training-free box-constrained diffusion. In *Proceedings of the IEEE/CVF International Conference on Computer Vision*, pages 7452–7461, 2023. [2](#)
- [70] Jinheng Xie, Weijia Mao, Zechen Bai, David Junhao Zhang, Weihao Wang, Kevin Qinghong Lin, Yuchao Gu, Zhijie Chen, Zhenheng Yang, and Mike Zheng Shou. Show-o: One single transformer to unify multimodal understanding and generation. In *The Thirteenth International Conference on Learning Representations*, 2025. [2](#), [4](#)
- [71] Jiazhen Xu, Xiao Liu, Yuchen Wu, Yuxuan Tong, Qinkai Li, Ming Ding, Jie Tang, and Yuxiao Dong. Imagereward: Learning and evaluating human preferences for text-to-image generation. *Advances in Neural Information Processing Systems*, 36, 2024. [2](#)
- [72] An Yang, Anfeng Li, Baosong Yang, Beichen Zhang, Binyuan Hui, Bo Zheng, Bowen Yu, Chang Gao, Chengen Huang, Chenxu Lv, et al. Qwen3 technical report. *arXiv preprint arXiv:2505.09388*, 2025. [2](#)
- [73] Ling Yang, Zhaochen Yu, Chenlin Meng, Minkai Xu, Stefano Ermon, and CUI Bin. Mastering text-to-image diffusion: Recaptioning, planning, and generating with multimodal llms. In *Forty-first International Conference on Machine Learning*, 2024. [1](#), [2](#), [3](#)
- [74] Michal Yarom, Yonatan Bitton, Soravit Changpinyo, Roei Aharoni, Jonathan Herzig, Oran Lang, Eran Ofek, and Idan Szepesktor. What you see is what you read? improving text-image alignment evaluation. *Advances in Neural Information Processing Systems*, 36, 2024. [2](#)
- [75] Junyan Ye, Dongzhi Jiang, Zihao Wang, Leqi Zhu, Zhenghao Hu, Zilong Huang, Jun He, Zhiyuan Yan, Jinghua Yu, Hongsheng Li, et al. Echo-4o: Harnessing the power of gpt-4o synthetic images for improved image generation. *arXiv preprint arXiv:2508.09987*, 2025. [1](#), [2](#), [7](#)
- [76] Xinchun Zhang, Ling Yang, Yaqi Cai, Zhaochen Yu, Kaini Wang, Jiake Xie, Ye Tian, Minkai Xu, Yong Tang, Yujiu Yang, and Bin Cui. Realcompo: Balancing realism and compositionality improves text-to-image diffusion models. *Advances in Neural Information Processing Systems*, 2024. [1](#), [2](#)
- [77] Chunting Zhou, Lili Yu, Arun Babu, Kushal Tirumala, Michihiro Yasunaga, Leonid Shamis, Jacob Kahn, Xuezhe Ma, Luke Zettlemoyer, and Omer Levy. Transfusion: Predict the next token and diffuse images with one multi-modal model. *arXiv preprint arXiv:2408.11039*, 2024. [2](#)
- [78] Xingyi Zhou, Vladlen Koltun, and Philipp Krähenbühl. Simple multi-dataset detection. In *Proceedings of the IEEE/CVF conference on computer vision and pattern recognition*, pages 7571–7580, 2022. [1](#)

Guiding What *Not* to Generate: Automated Negative Prompting for Text-Image Alignment

Supplementary Material

A. Additional Benchmark

T2I-CompBench T2I-CompBench [20] provides compositional prompts with multiple objects. We evaluate six tasks—attribute binding (color, shape, texture), object relationships (spatial, non-spatial), and a complex setting combining them—using 300 images per task (1,800 total). Metrics follow the benchmark: BLIP-VQA [20] for attribute binding, UniDet [78] for spatial relations, and CLIPScore [15, 51] for non-spatial relations; all three are applied to the complex task. In this setup, we compare our approach against recent alignment-enhancing methods in three groups: (1) *attention map-based* (Attend-and-Excite [4], SynGen [53]); (2) *layout-based* (LMD [32], InstanceDiffusion [61]); and (3) *feedback-based* (GORS [20], CoMat [23]). Only Attend-and-Excite is implemented on Stable Diffusion 2; the others (and ours) are implemented on SDXL.

In this experiment, we implement NPC on SDXL for a fair comparison. As shown in Table S3, NPC attains the best attribute-binding performance and nearly a 15%p gain on the complex task. While layout-based methods improve spatial controllability, their dependence on LLM outputs leads to failures with small or overlapping boxes [46]. In contrast, NPC avoids these issues, requires no additional training (unlike feedback-based methods), and needs no gradient updates (unlike attention-based methods), yielding both efficiency and superior average performance across tasks. Qualitative samples of alignment methods are also provided in Figure S2.

DPG-Bench DPG-Bench [18] comprises 1,065 long, dense prompts designed for compositional text-image evaluation, drawn from COCO, PartiPrompts, DSG-1k, and Objects365 and expanded via GPT-4, then human-verified (5 level-1 and 13 level-2 categories). DPG-Bench assesses text-to-image models on complex prompts, using mPLUG-large [29] to evaluate entities, attributes, and relationships with a focus on fine-grained details like object properties and spatial arrangements.

Table S4 reports DPG-Bench results: NPC attains state-of-the-art relation accuracy (93.34) and the highest overall score, while remaining strong on entities. It lags top systems on global/other and is slightly behind on attributes, yet still captures fine-grained compositional details efficiently. Figure S3 further shows robust alignment in complex scenes.

	pre-check	caption	propose	salient score
Time (s)	2.77	4.55	0.78	23.48

Table S1. Computation time by stage.

B. Experimental Details

Software and Hardware All experiments used PyTorch and an NVIDIA A40 GPU.

Inference time and Memory Results averaged over 10 randomly sampled cases (as in Table S1): pre-check about 2.77 s, caption about 4.55 s, proposal about 0.78 s, and scoring about 23.48 s. Scoring is the longest stage, but the overall increase remains marginal in practice. Memory changes were only marginal: we use the GPT API for captioning/proposal (no local GPU growth), and the salient-score stage ran on CPU, so GPU usage remained effectively unchanged.

C. Additional Results for Section 3

For further validation of our analysis in Section 3, we compute salient attention scores on a broader set of prompts, as summarized in Table S5. Salient tokens are manually selected from the generated images to pinpoint regions where text-image alignment fails; this manual curation is necessary to precisely measure how much attention increases on the misaligned parts, providing a more rigorous and reliable verification of our analysis. Across ten additional prompts, both the targeted and untargeted settings consistently yield higher salient attention scores than the base, reinforcing the robustness of our findings.

D. Model-Agnostic Effectiveness of NPC

To assess the generality of NPC beyond a single model or component choice, we evaluate its effectiveness across diverse generative architectures and MLLM or LLM configurations. As shown in Table S6, across all three base models—SDXL [49], SD3 [11], and FLUX [26]—applying NPC consistently improves performance on every evaluated attribute. The gains are substantial and uniform, demonstrating that NPC is not model-specific but transfers effectively across architectures with different capacities. These results confirm the general robustness and broad applicability of NPC.

Method	Attribute Binding			Object Relationship		Complex \uparrow	AVG \uparrow
	Color \uparrow	Shape \uparrow	Texture \uparrow	Spatial \uparrow	Non-Spatial \uparrow		
DPO-Diff [60]	0.4405	0.4381	0.4949	0.1445	0.3182	0.4119	0.3746
NPC_{SDXL}	0.7950	0.5681	0.6889	0.2545	0.3191	0.5171	0.5237

Table S2. Comparison with negative prompt optimization method (Section E).



Figure S1. Examples of DPO-Diff (Section E).

We further evaluate NPC using an alternative component stack in which the verifier and captioner are implemented with Qwen2.5-VL [2] and the proposer with Qwen3 [72]. As shown in Table S7, the Qwen-based configuration achieves performance comparable to the GPT-based setup across all attributes, demonstrating that NPC remains effective even when substituting the underlying LLM components. This again highlights the model-agnostic nature of NPC and its robustness across different verifier, captioner, and proposer architectures.

E. Comparison with Negative Prompt Optimization Method

Many prompt optimization approaches for enhancing image quality have been explored [14, 40]. Since NPC can also be considered a negative prompt optimization method, we compare it with DPO-Diff [60], a recently proposed approach that designs a compact space and employs shortcut gradient search to optimize negative prompts. As shown in Table S2, NPC outperforms DPO-Diff in T2I-CompBench since DPO-Diff is not specifically designed for alignment (examples of negative prompts from DPO-Diff are provided in Figure S1). Moreover, unlike DPO-Diff, which requires training, NPC enhances alignment purely through inference, making it a more efficient alternative.

F. LLM Prompts

In Table S8, Table S9, and Table S10, we provide the full LLM prompts used for the verifier, captioner, and proposer. Table S11 shows the LLM prompt used in the ablation study of the prompt-only proposer in Section 5.3.

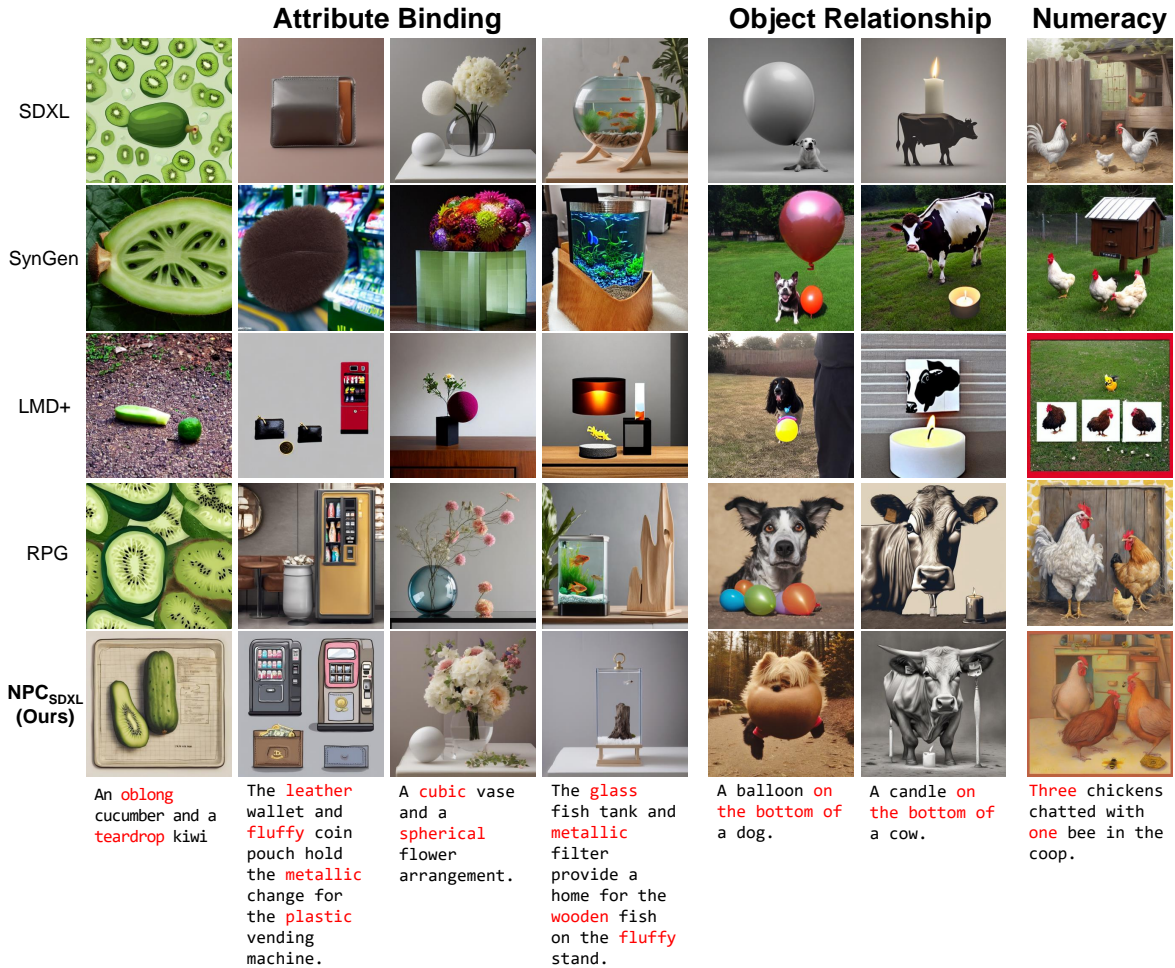


Figure S2. Qualitative comparison with SDXL [49] and other text-image alignment methods [32, 53, 73]. NPC consistently aligns across various tasks, while other methods fail in some tasks. Samples for NPC are generated using SDXL.

Model	Attribute Binding			Object Relationship		Complex ↑	AVG ↑
	Color ↑	Shape ↑	Texture ↑	Spatial ↑	Non-Spatial ↑		
Stable Diffusion 2	0.5065	0.4221	0.4922	0.1342	0.3096	0.3386	0.3672
SDXL	0.6369	<u>0.5408</u>	0.5637	0.2032	0.3110	0.4091	0.4441
● Attn-Exct v2	0.6400	0.4517	0.5963	0.1455	0.3109	0.3401	0.4140
● SynGen	0.7000	0.4550	0.6010	0.2260	0.3100	0.3339	0.4376
● LMD	0.4814	0.4865	0.5699	0.2537	0.2828	0.3323	0.4011
● InstanceDiffusion	0.5433	0.4472	0.5293	0.2791	0.2947	0.3602	0.4089
● GORS	0.6603	0.4785	0.6287	0.1815	0.3193	0.3328	0.4335
● CoMat	<u>0.7827</u>	0.5329	<u>0.6468</u>	0.2428	0.3187	<u>0.3680</u>	<u>0.4819</u>
NPC_{SDXL} (Ours)	0.7950	0.5681	0.6889	<u>0.2545</u>	<u>0.3191</u>	0.5171	0.5237

Table S3. T2I-CompBench. Comparison of various methods across different attributes. The best performances are highlighted in bold and the second-best are underlined. The red circle (●) represents attention-map-based approaches, the blue circle (●) indicates layout-based approaches, and the green circle (●) denotes feedback-based approaches. Performance for the baselines is based on reported values.

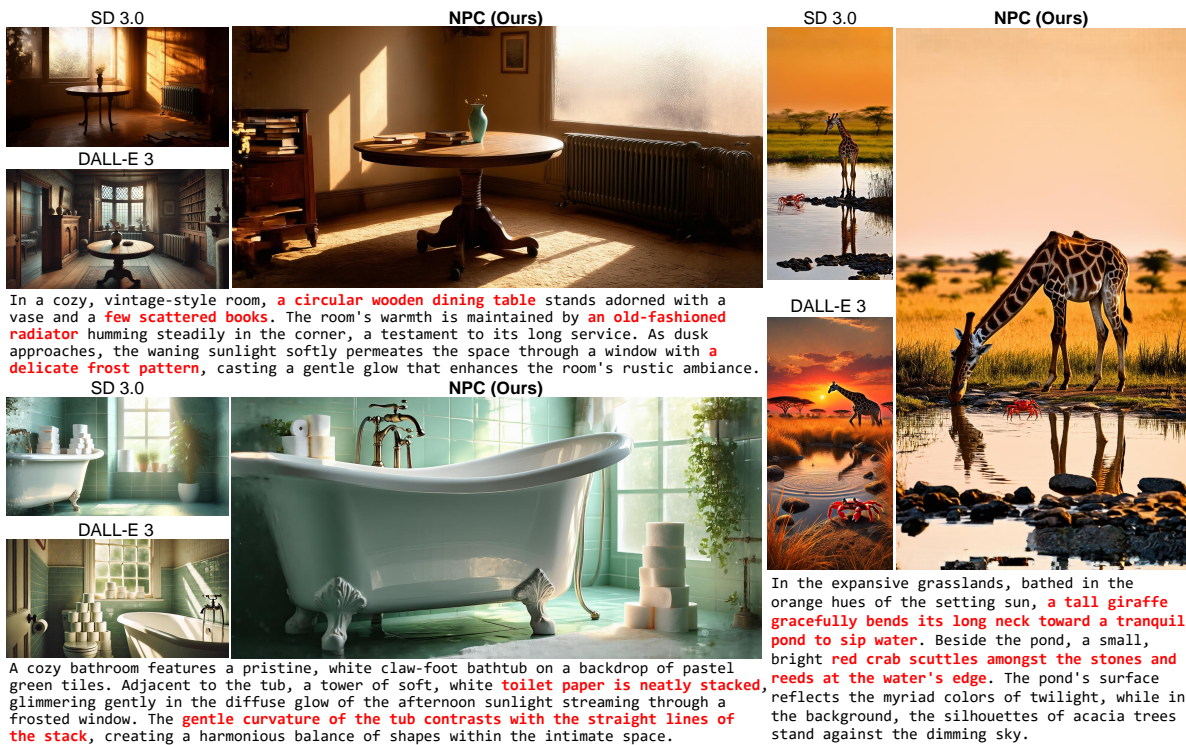


Figure S3. Examples using DPGBench, comparing NPC with SD3.0 and DALL-E 3, demonstrate that NPC is also effective for long, dense-context prompts. Quantitative comparison results are provided in the Table S4.

Method	Global \uparrow	Entity \uparrow	Attribute \uparrow	Relation \uparrow	Other \uparrow	Overall \uparrow
SDXL [49]	83.27	82.43	80.91	86.76	80.41	74.65
Hunyuan-DiT [31]	84.59	80.59	88.01	74.36	86.41	78.87
DALLE3 [3]	<u>90.97</u>	89.61	88.39	90.58	<u>89.83</u>	83.50
SD3-medium [11]	87.90	<u>91.01</u>	88.83	80.70	88.68	84.08
FLUX.1-dev [26]	82.10	89.50	88.70	<u>91.10</u>	89.40	84.00
OmniGen [68]	87.90	88.97	88.47	87.95	83.56	81.16
Show-o [70]	79.33	75.44	78.02	84.45	60.80	67.27
EMU3 [62]	85.21	86.68	86.84	90.22	83.15	80.60
TokenFlow-XL [50]	78.72	79.22	81.29	85.22	71.20	73.38
Janus Pro [7]	86.90	88.90	89.40	89.32	89.48	84.19
T2I-R1 [24]	91.79	90.23	89.05	90.13	89.48	84.76
UniWorld-V1 [34]	83.64	88.39	88.44	89.27	87.22	81.38
OmniGen2 [65]	88.81	88.83	<u>90.18</u>	89.37	90.27	83.57
BAGEL [10]	88.94	90.37	91.29	90.82	88.67	<u>85.07</u>
NPC_{FLUX}	83.88	91.12	87.69	93.34	83.03	85.38

Table S4. DPG-Bench comparison (higher is better, \uparrow). Bold indicates the best value in each column; underline indicates the second-best.

Prompt	Salient	Targeted	Untargeted	Base \uparrow	Targeted \uparrow	Untargeted \uparrow
A photo of two trains, three bottles, and two tennis rackets	three	2 bottles	toy stream locomotives	0.0831	0.1018	0.0839
					+0.0187	+0.0008
A photo of three bowls and two apples	three	stacked bowls	shiny apples	0.0746	0.1018	0.0860
					+0.0272	+0.0114
A photo of two teddy bears and three laptops	three	one laptop	wooden table	0.0583	0.0642	0.0703
					+0.0059	+0.0120
A photo of a purple chair, a blue bottle, and a white vase	white	purple vase	bulbous object	0.0427	0.0512	0.0473
					+0.0085	+0.0046
A photo of a larger donut on the above and a smaller zebra on the below	zebra	two donuts	colorful sprinkles	0.0344	0.0371	0.0428
					+0.0027	+0.0084
A photo of seven bears	seven	six bears	wildflowers	0.0926	0.1031	0.1070
					+0.0105	+0.0144
A photo of six vases	six	seven vases	glass vases	0.0863	0.0947	0.0963
					+0.0084	+0.0100
A photo of three dining tables and three horses	three	two horses	chandelier	0.1571	0.1638	0.1630
					+0.0067	+0.0059
A photo of two stop signs and one birds	two	one stop sign	television sets	0.0790	0.0850	0.0820
					+0.0060	+0.0030
A photo of two green tvs and two pink potted plant	two	one green TV	antennas	0.1178	0.1464	0.1289
					+0.0286	+0.0111

Table S5. Additional results for Section 3. results (higher is better, \uparrow). In each pair of rows, the first row lists *Base*, *Targeted*, and *Untargeted* scores (cells in **green, bold** exceed *Base*); the second row shows unlabeled absolute improvements in the last two columns (*Targeted*–*Base*, *Untargeted*–*Base*). All prompts show *Targeted* and *Untargeted* > *Base*.

Model	Color	Count	Color/Count	Color/Pos	Pos/Count	Pos/Size	Multi-Count	Overall
SDXL [49]	0.050	0.375	0.000	0.000	0.000	0.000	0.000	0.061
NPC _{SDXL}	0.500	0.575	0.200	0.400	0.325	0.425	0.500	0.417
SD3 [11]	0.550	0.500	0.125	0.350	0.175	0.150	0.225	0.296
NPC _{SD3}	0.650	0.675	0.325	0.550	0.575	0.600	0.625	0.571
FLUX [26]	0.350	0.625	0.150	0.275	0.200	0.375	0.225	0.314
NPC _{FLUX}	0.550	0.675	0.350	0.525	0.550	0.725	0.625	0.571

Table S6. Comparison of metric scores across three models before and after applying NPC. In all cases, NPC improves performance across all evaluated attributes.

Method	Color	Count	Color/Count	Color/Pos	Pos/Count	Pos/Size	Multi-Count	Overall
Qwen	0.650	0.575	0.400	0.500	0.575	0.650	0.600	0.564
GPT	0.550	0.675	0.350	0.525	0.550	0.725	0.625	0.571

Table S7. Comparison of metric scores between Qwen-based and GPT-based components for NPC.

<System Prompt>: You are an expert image evaluator.

Decide if a single candidate image fully satisfies a natural-language INSTRUCTION and, if provided, an expectation CHECKLIST.

Strict rules:

- 1) All expectations must be satisfied:
 - Object classes, counts, colors, spatial relations (above/below/left/right by pixel position), size/relative scale.
- 2) The image must be a single coherent, natural, photo-like scene.
 - Reject stylized (cartoons, sketches, anime), collages, multi-panels, or text-only.
- 3) Be strict and conservative. If uncertain, mark incorrect.

Return a strict JSON object only:

```
{"correct": 1 or 0, "score": float in [0,1], "reason": "brief explanation"}
```

No extra text. "score" should reflect how well the image meets the INSTRUCTION (and CHECKLIST), even if correct=0.

<User Prompt>: POSITIVE PROMPT:

```
$positive_prompt
```

CHECKLIST (optional):

```
$checklist
```

Judge the attached image against the INSTRUCTION (and CHECKLIST if present).

Return exactly:

```
{"correct": 1 or 0, "score": float in [0,1], "reason": "brief explanation"}
```

Table S8. LLM prompt for *Verifier*.

<System Prompt>: You are a meticulous visual describer.

Write a comprehensive caption (90--160 words) describing concrete, falsifiable details only.

Cover: main objects (counts, colors, materials), textures/patterns, spatial relations, background elements,

lighting, style/mood, any visible text.

Avoid speculation, emotions, and camera metadata. Output plain text only.

<User Prompt>: Describe this image.

Table S9. LLM prompt for *Captioner*.

<System Prompt>: You are a precise prompt editor.
From a given POSITIVE PROMPT and an image CAPTION, extract concise negative prompt candidates (1--6 words, all lowercase) that would most effectively steer generation away from elements that contradict the POSITIVE PROMPT.
Return a strict JSON object as specified. Do not include explanations.

<User Prompt>: POSITIVE PROMPT:
\$positive_prompt

CAPTION:
\$caption

GENERAL_FALLBACKS (use only if needed to reach K):
\$fallbacks

K (max total candidates): \$k

Task

- 1) From the CAPTION, find elements that are NOT requested by the POSITIVE PROMPT (consider synonyms, inflections, paraphrases).
- 2) Prioritize contradictions to the POSITIVE PROMPT (object identity, attributes like color/material/count/shape, relations/pose), and if contradictions are weak or absent, pick items at least tightly related to the POSITIVE PROMPT's objects (foreground-first).
- 3) Produce a flat list "candidates" of up to K concise negative phrases.
- 4) If you have fewer than K items, supplement with the most relevant items from GENERAL_FALLBACKS while still obeying all constraints and avoiding anything implied by the POSITIVE PROMPT.
- 5) Return exactly K items if possible (use fallbacks to fill). Only return fewer than K if no valid item remains.

Constraints

- Use ONLY elements explicitly present in the CAPTION.
- Exclude anything present in (or synonymous with) the POSITIVE PROMPT.
- Phrases: lowercase, 1--6 words, no "no/without/not", no quotes, no trailing punctuation, no duplicates.

Return exactly:
{"candidates": ["...", "...", "..."]}

Table S10. LLM prompt for *Proposer*.

<System Prompt>: You are a precise prompt editor.
Given only a POSITIVE PROMPT (no caption) and K, produce up to K concise negative prompt candidates (1--6 words, all lowercase) that would most effectively steer image generation away from elements that contradict the POSITIVE PROMPT.
Return only strict JSON as specified. Do not include explanations.

Task

- 1) Parse the POSITIVE PROMPT to identify primary subjects/objects, key attributes (color/material/count/shape/pose), relations, scene/setting/time/lighting, viewpoint/composition, and medium/style/era.
- 2) Generate concise negative phrases that capture the most likely contradictions or near-misses to those elements, prioritized in this order: foreground object identity → attributes → relations/pose → composition/viewpoint → style/medium/era.
- 3) If strong contradictions are scarce, choose tightly related alternatives for the same foreground objects (e.g., sibling species, alternate colors/counts, opposite angles).

Constraints

- Phrases: lowercase, 1--6 words, no ``no/without/not'', no quotes, no trailing punctuation, no duplicates.
- Exclude anything present in (or synonymous with) the POSITIVE PROMPT.
- Use only concepts reasonably inferred from the POSITIVE PROMPT's domain; avoid unrelated items.
- Foreground-first: prefer conflicts about the main subject before background or style.

<User Prompt>: POSITIVE PROMPT: \$positive_prompt

K (max total candidates): \$k

Task:

Propose \$k negative prompt tokens likely to reduce undesirable or off-topic elements that could appear when generating this scene.

Return exactly:

```
{"candidates": ["...", " ..."]}
```

Table S11. LLM prompt for prompt ablation in Section 5.3.